Available online at www.sciencedirect.com

ScienceDirect

Procedia Structural Integrity 42 (2022) 58–65

Structural Integrity Procedia

www.elsevier.com/locate/procedia

23 European Conference on Fracture - ECF23

PBF-LB/M/316L vs. hot-rolled 316L – comparison of cyclic plastic material behavior

Johannes Diller[a]*, Dorina Siebert[a], Christina Radlbeck[a], Martin Mensinger[a]

a) Chair of Metal Structures, Technical University of Munich, Arcisstr. 21, 80333 Munich, Bavaria, Germany

Abstract

Powder-Bed Fusion of AISI 316L (1.4404) using a laser (PBF-LB/M) is known for its very high cooling rate of up to 40 K/µs (Hooper 2018). This high cooling rate results in a fine needle-like microstructure. In comparison, hot-rolled, annealed AISI 316L consists of coarser grain structures. The quasi-static tensile properties, therefore, differ significantly. This may result in a completely different cyclic plastic material behavior due to the grain boundary strengthening during the PBF-LB/M manufacturing process.
This study compares the cyclic plastic material behavior of PBF-LB/M-manufactured 316L with that of hot-rolled, annealed AISI 316L. Strain-controlled fatigue testing of both, PBF-LB/M and hot rolled, annealed AISI 316L, was conducted. The strain amplitudes vary from 0.5 % to 3.0 % in steps of 0.5 %. A microstructural investigation of selected specimens was conducted before and after testing. It consists of surface etching, electron backscatter diffraction (EBSD) as well as spark spectrometry. The orientation, phase transformation, twinning formation as well as the general microstructure is compared.
It is found, that the PBF-LB/M-manufactured specimens mainly showed a softening behavior. Only from 2.5 % applied strain amplitude, a secondary hardening phenomenon is observed. The hot-rolled and annealed specimens on the other hand mainly show a continuous hardening behavior.

Keywords: Low-cycle fatigue, Additive Manufacturing, AISI 316L, Hot-rolling, Strain hardening, Cyclic plastic material behavior

* Corresponding author. Tel.: +49 89 289 22528; fax: +49 89 289 22522
E-mail address: johannes.diller@tum.de

10.1016/j.prostr.2022.12.006

1. Introduction

Laser powder bed fusion of metals (PBF-LB/M) enables the production of highly complex parts which can, in many situations, not be manufactured by conventional manufacturing methods like casting or forging. However, the mechanical properties of PBF-LB/M manufactured parts are not yet fully understood or characterized. Often, the austenitic stainless steel AISI 316L is used to gain more knowledge about the PBF-LB/M manufacturing process (Gor et al. 2021). 316L is mainly used for chemical, medical and automotive applications (Afkhami et al. 2021). It could however also be used in the construction industry as a structural steel for special applications like steel hysteretic dampers due to its high ductility. For conventional manufacturing methods like forging, the yield strength usually lies in between 200 – 220 MPa (Ravi Kumar 2010). The yield strength of PBF-LB/M manufactured 316L however can rise up to 650 MPa, depending on the orientation of the part and the applied laser parameters (Diller et al. 2020). The high yield strength results from a grain boundary strengthening, which is caused by the high cooling rate (Liu et al. 2020). During the PBF-LB/M manufacturing, cooling rates of up to 40 K/µs can occur (Hooper 2018). This creates fine lamellar subgrains with a diameter of 200 – 300 nm. Hence, the higher yield strength of PBF-LB/M manufactured 316L can be attributed to the inhibition of dislocation motion at each grain boundary. With a smaller subgrain size, more grain boundaries occur, developing a high yield strength. (Diller et al. 2022). This study compares the cyclic plastic material behavior of PBF-LB/M-manufactured and hot-rolled AISI 316L. The cyclic plastic material behavior of additively manufactured 316L was investigated in detail in a different study and was compared to a different laser parameter set which was outside the stable melting zone (Diller et al. 2022). For each manufacturing process, strain-controlled fatigue testing was conducted with strain amplitudes of up to 3.0 % with steps of 0.5 %. Tensile testing, as well as a microstructural investigation before and after testing was conducted.

2. Experimental procedure

An EOS M280 PBF-LB/M machine with a 400 W Ytterbium continuous wave fiber laser was used to manufacture the PBF-LB/M specimens for this study. AISI 316L stainless steel metal powder by Oerlikon Metco with a particle size distribution of 20 – 63 µm was used. The respective volume percentile values D10, D50 and D90 were numerated with 19, 30 and 40 µm respectively. The used inert gas was Argon 5.0. During the build job, a residual oxygen concentration of < 1300 ppm was kept. The laser parameters used in this study are shown in Table 1. According to (Yakout et al. 2019) the used laser parameters are inside the stable melting zone. The application of these laser parameters should therefore result in a high density and toughness with continuous weld beads and homogeneous melt tracks. The x-hatch angle was kept at 60° after each layer.

Table 1: Applied laser parameters of the PBF-LB/M manufactured for the fatigue and tensile specimens

Energy Density [J/mm³]	Scanning Velocity [mm/s]	Laser Power [W]	Layer Thickness [µm]	Hatch Distance [µm]
65.97	600	190	40	120

Strain-controlled fatigue testing was conducted with a strain ratio of R = -1 and a strain rate of 0.004 s^{-1}. Additionally, tensile tests were conducted with the same specimen geometry according to ASTM E606, shown in Fig. 1, to reduce any geometrical effect. The experimental design can be seen in Table 2.

Table 2: Experimental design with type and number of specimens for each conducted type of investigation and process

Manufacturing Process	Applied Strain Amplitude						Tensile Testing	Microstructure
	0.5 %	1.0 %	1.5 %	2.0 %	2.5 %	3.0 %		
PBF-LB/M	3	3	3	3	3	3	3	1
Hot-rolled	3	3	3	3	3	3	3	1

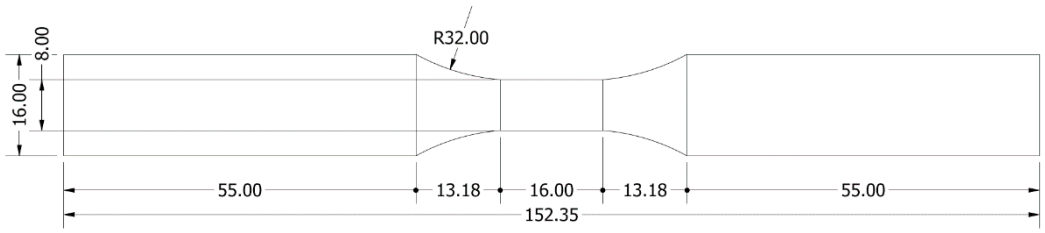

Fig. 1. Fatigue and tensile specimen geometry (round) with dimensions in mm according to ASTM E606

The unique surface roughness of PBF-LB/M manufactured AISI 316L may affect the low-cycle fatigue behavior (AS et al. 2008; Solberg et al. 2019; ITOGA et al. 2005). To diminish the effect of surface roughness on the low-cycle fatigue behavior, both PBF-LB/M and hot-rolled AISI 316L specimens were ground and polished on a lathe. Sanding papers with a grain size of 320, 500, 800 and 1000 µm were used for 4 minutes each, followed by two polishing steps. For this, zirconia aluminum abrasive and a polishing paste with 6 µm and 3 µm diamond slurry was applied. The polishing steps were applied for 5 minutes each. Subsequently, the surface roughness was measured with a Keyence VK-X1000 3D laser scanning microscope resulting in an Ra = 0.562 µm and Rz = 4.326 µm. The microstructure was investigated before and after testing by cutting the specimens longitudinally inside the measuring range. The specimens were hot embedded in resin, ground, polished and etched for 30s. The used etchant was Beraha II as well as V2A-etchant at 60 °C. The ferrite content was measured before and after testing with a Fischer Feritscope FMP30. The Feritscope was calibrated using a calibration block with a ferrite content of 0.3 % and 10 %. Electron backscatter diffraction (EBSD) measurements were conducted to investigate the phase composition, as well as the possible formation of twins and the orientation of the material. Therefore, an EDAX EBSD-system and a Hikari EBSD-camera was used. The overall chemical composition was investigated using an OBFL QSG 750-II spark spectrometer.

3. Experimental results

3.1. Chemical composition

The chemical composition of the AISI 316L of both manufacturing processes is shown in Table 3. It can be seen, that the Ni-content is at the lower spectrum for hot-rolled AISI 316L. The Ni-content of the PBF-LB/M manufactured AISI 316L however is at the upper end of the defined range (Wegst 2001).

Table 3: Chemical composition of 316L, manufactured by PBF-LB/M and hot-rolling in % including the range AISI 316L is defined (Wegst 2001).

Chemical Element	C	Si	Mn	Cr	Ni	Nb	Ti	Mo
PBF-LB/M	0.015	0.582	1.349	17.85	12.0	0.011	<0.001	2.277
Hot-rolled	0.035	0.41	1.52	17.01	10.02	0.019	<0.001	2.021
Range	<0.03	<1.0	<2.0	16.5-18.5	10.0-13.0			2.0-2.5

3.2. Tensile properties

Fig. 2 shows the tensile testing results of both PBF-LB/M manufactured and hot-rolled AISI 316L. The PBF-LB/M manufactured AISI 316L showed a higher yield strength of 455 MPa in comparison to the hot-rolled AISI 316L with a yield strength of 245 MPa respectively. The ultimate tensile strength revealed closer results with 611 MPa for the PBF-LB/M manufactured AISI 316L and 585 MPa for the hot-rolled AISI 316L respectively. It can also be seen, that

both manufacturing processes resulted in different strengthening mechanisms. The PBF-LB/M manufactured AISI 316L showed a plateau in the plastic range whereas the hot-rolled AISI 316L hardened during plastic deformation

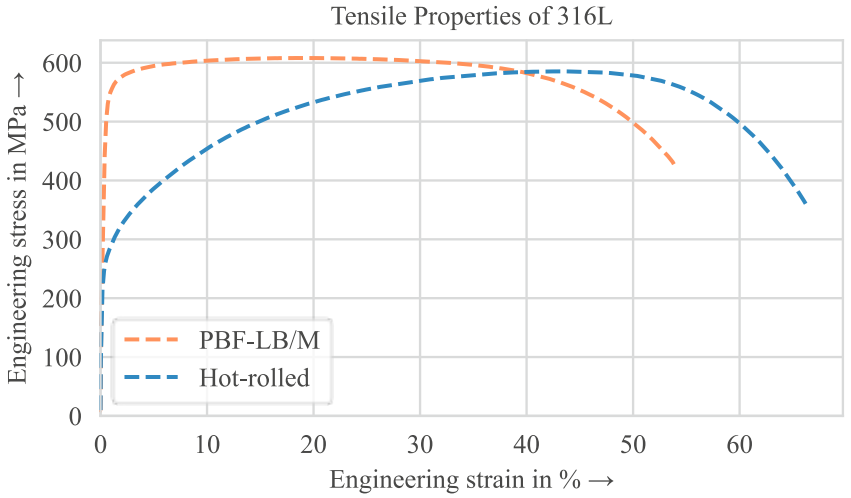

Fig. 2: Tensile properties of AISI 316L, manufactured by PBF-LB/M and hot-rolling

3.3. Microstructure before testing

The microstructure of the PBF-LB/M manufactured and hot-rolled AISI 316L is shown in Fig. 3. The weld beads revealed the x-scan strategy of 60 ° in picture (1). It also revealed the subgrain size. Columnar grains with a diameter of 400-600 nm were visible. The subgrains were oriented differently to each other, depending on the scan angle. In picture (2) the microstructure of the hot-rolled AISI 316L revealed larger grains with a diameter of up to 192 µm. Initial twinning was visible. A ferrite content of 0.0 % was measured for the PBF-LB/M manufacturing process and 0.3 % for the hot-rolling process respectively.

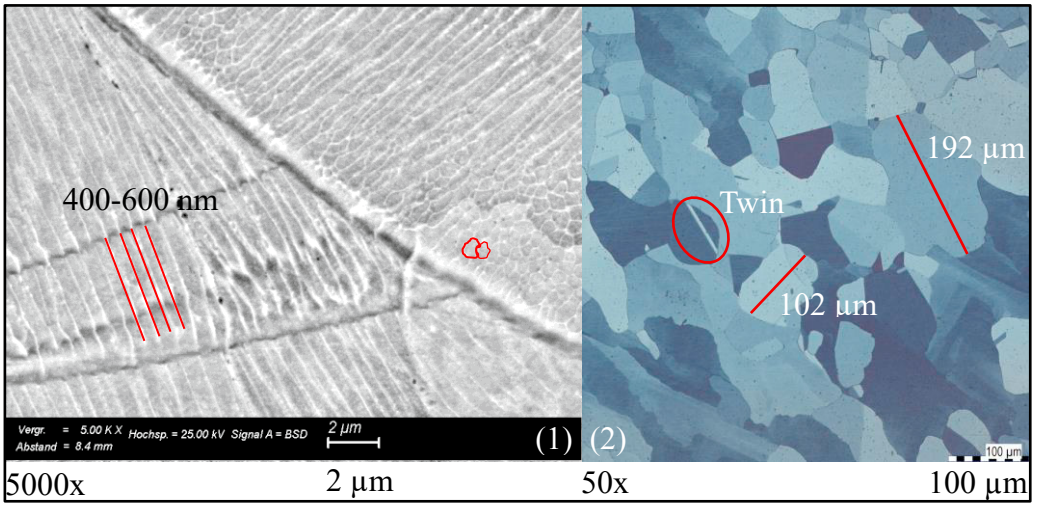

Fig. 3: Microstructure of both PBF-LB/M (1) manufactured and hot-rolled (2) AISI 316L, (1) showing columnar grains with a diameter of 400 – 600 nm and (2) showing twins and grains with a diameter of up to 192 µm.

3.4. Strain-controlled fatigue testing

Fig. 4 shows the results of the strain-controlled fatigue testing of the specimens of both the PBF-LB/M and the hot-rolling processes. A comparison of the maximum stresses in the tensile range is conducted. The PBF-LB/M manufacturing process results showed high initial stresses during cyclic plastic deformation. An initial hardening effect in the first 10 cycles was observed, followed by secondary softening during the whole fatigue life. Only from a strain amplitude of 2.5 % upwards, a hardening effect occurred close to the end of the fatigue life of the specimen.

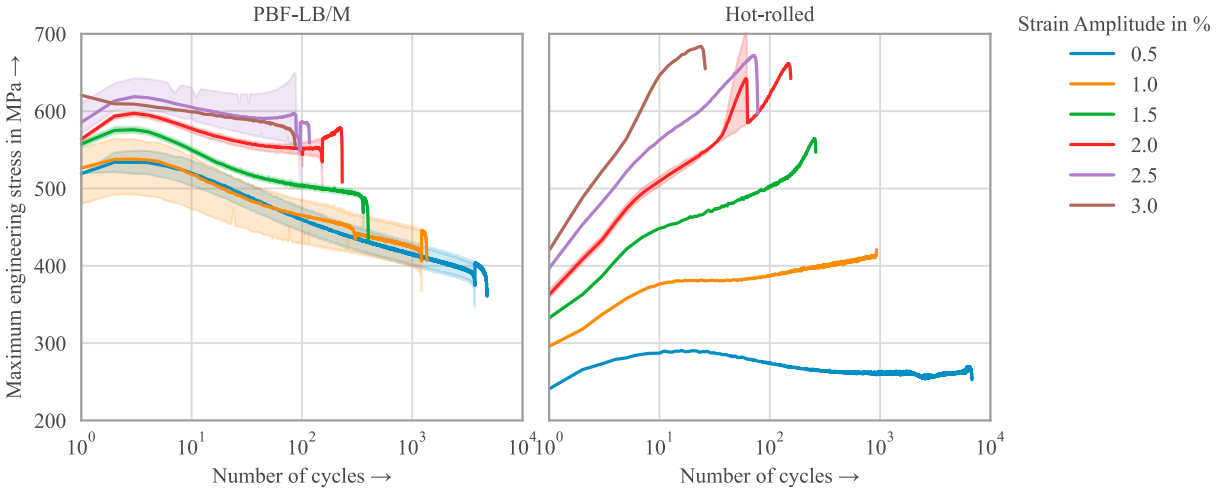

Fig. 4: Comparison of the maximum stress curves over the endured cycles between the PBF-LB/M manufacturing process and the hot-rolling process of AISI 316L including the standard deviation at each cycle (colored surfaces).

The specimens of hot-rolled AISI 316L showed low initial stresses, followed by an initial hardening behavior during cyclic plastic deformation. This hardening behavior continues through to the end of the fatigue life. Stresses of up to 700 MPa were generated. The strain-based S-N-curve for both the PBF-LB/M manufacturing process and the

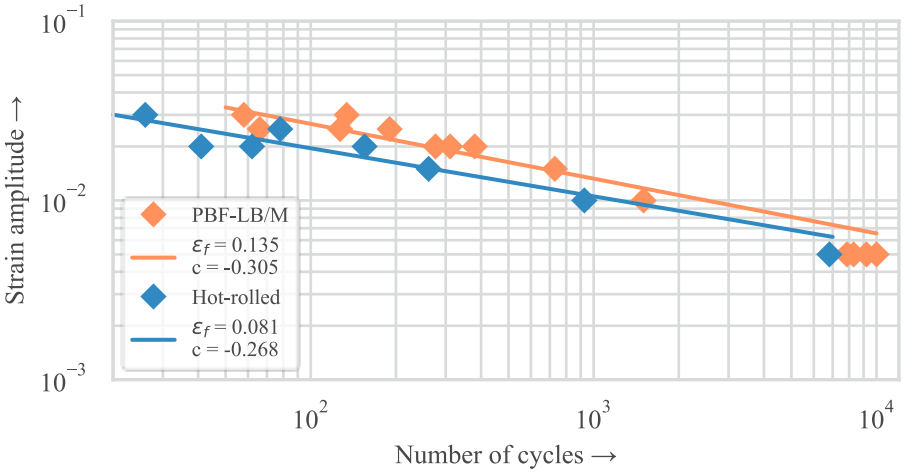

Fig. 5: Linear regression approximation of the plastic strain-based S-N-curve for the PBF-LB/M manufacturing process and the hot-rolling process of AISI 316L.

hot-rolling process are described with the plastic part of the Manson-Coffin equation in Fig. 5. The PBF-LB/M manufactured AISI 316L has a higher fatigue life compared to the hot-rolled AISI 316L.

3.5. Microstructure after fatigue testing with 2.5 % strain amplitude

The microstructure was investigated after the application of 2.5 % strain amplitude for both manufacturing processes. The twin formation was measured by EBSD. The orientation between 58° and 62° is shown in Fig. 6 (1) and (2) as this is the usual angle where twinning occurs (Brust et al. 2019; Guo et al. 2017). A twin fraction of 2.2 % was measured for the PBF-LB/M manufactured AISI 316L after applying 2.5 % strain amplitude, see Fig. 6 (1). The twin fraction of the hot-rolled AISI 316L after fatigue testing with 2.5 % strain amplitude however shows a substantially higher twin fraction of 10.2 %. Additionally, the phase fraction was measured by EBSD. For the PBF-LB/M manufactured AISI 316L no martensite was measured before and after an applied strain amplitude of 2.5 %. The hot-rolled AISI 316L however shows a martensite fraction of 11.5 % which can be seen in Fig. 6 (3). The ferrite content was also measured after an applied strain amplitude of 2.5 %. The PBF-LB/M manufactured AISI 316L revealed a ferrite or martensite content of 0.31% whereas for the hot-rolled AISI 316L a ferrite content of 11.5 % was measured.

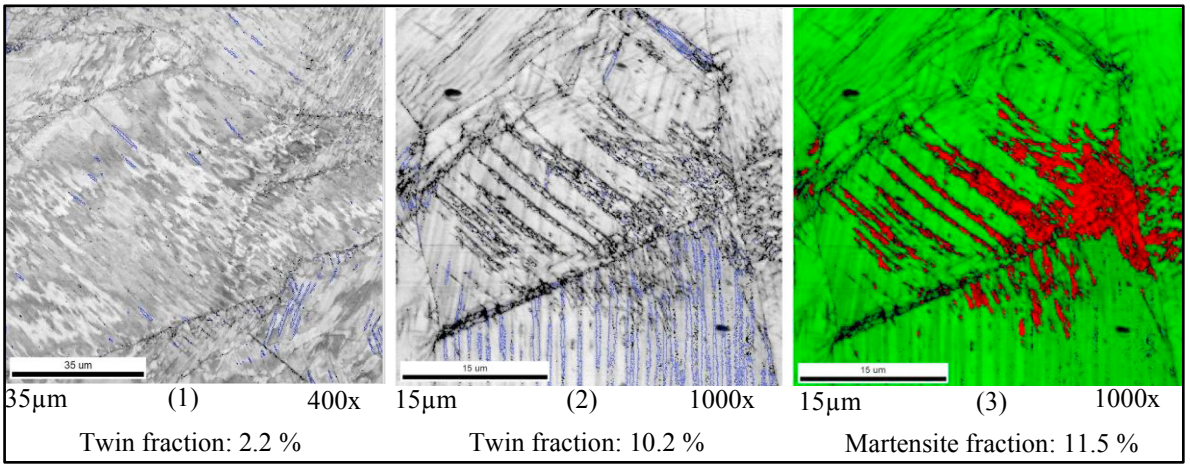

Fig. 6: Microstructure after fatigue testing with 2.5 % strain amplitude, (1) showing the mechanical twin formation and image quality of the PBF-LB/M manufactured AISI 316L, (2) showing the mechanical twin formation and image quality of the hot-rolled AISI 316L, (3) showing the phase composition of the hot-rolled AISI 316L with a martensite fraction of 11.5 %.

4. Discussion

The two different manufacturing processes reveal a completely different strengthening behavior. To investigate this behavior, Fig. 7 is introduced. The normalized number of cycles is compared to the change of the maximum tensile stress for each strain amplitude and both manufacturing processes. It can be seen, that at strain amplitudes from 0.5 % to 1 %, the PBF-LB/M manufactured AISI 316L constantly shows higher stresses. From 1.5 % strain amplitude onwards, a clear hardening effect of the hot-rolled AISI 316L is observed, exceeding the resulting stresses of the PBF-LB/M manufactured AISI 316L.

While the cyclic plastic behavior of the PBF-LB/M manufactured AISI 316L is mainly dominated by softening, the hot-rolled manufactured AISI 316L is mainly dominated by hardening. This may be due to multiple reasons. The chemical composition shows a lower Ni-content for the hot-rolled AISI 316L. This may lead to a higher transformation affinity from austenite to martensite, as the Ni-equivalent of the Schaeffler-diagram is lower (Schoß 2000). The grain size of the material also may have a significant influence on the strain induced martensite transformation. With increasing grain size, the transformation rate from austenite to martensite increases as well (Celada-Casero et al. 2019).

As martensite can only grow inside a grain due to their specific orientation relation with the austenite, it is very likely that the magnitude of the martensite transformation of the hot-rolled AISI 316L is higher in comparison to the PBF-LB/M manufactured AISI 316L. Additionally the strain induced twin formation is significantly higher at the hot-rolled AISI 316L in comparison to the PBF-LB/M manufactured AISI 316L.

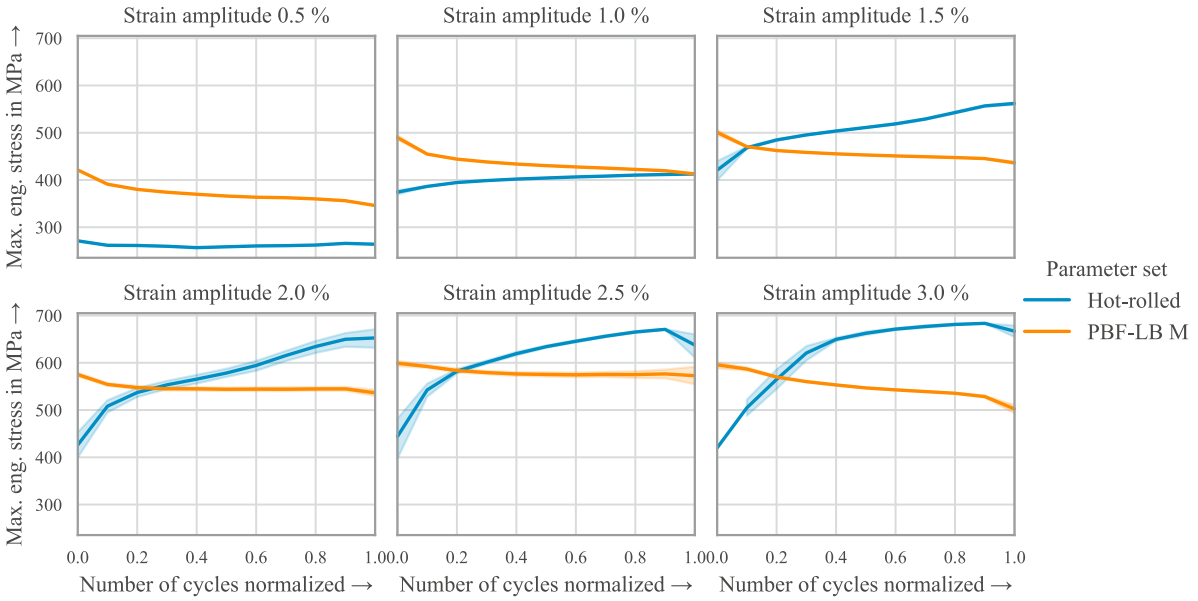

Fig. 7: Comparison of the maximum stress curves over the endured cycles between the PBF-LB/M manufacturing process and the hot-rolling process. The tested strain amplitudes are shown in separate plots with a normalized representation of the elapsed number of cycles.

5. Conclusion

From this study, the following conclusions can be drawn about the cyclic plastic material behavior of both PBF-LB/M manufactured and hot-rolled AISI 316L:

- The PBF-LB/M manufactured AISI 316L reveals higher initial maximum stresses, followed by a softening behavior.
- The hot-rolled AISI 316L has lower initial maximum stresses, followed by a hardening behavior.
- The PBF-LB/M manufactured AISI 316L has a higher fatigue life in comparison to hot-rolled AISI 316L.
- During cyclic plastic deformation of the PBF-LB/M manufactured AISI 316L, no to little martensite transformation occurs due to the small crystallite size.
- The martensite transformation during cyclic plastic deformation of the hot-rolled AISI 316L occurs due to the large grain size.
- The lower Ni-content of the hot-rolled AISI 316L leads to a higher transformation affinity from austenite to martensite.
- The hardening behavior of the hot-rolled AISI 316L can therefore be reasoned with both martensite transformation and strain induced twinning.

6. Acknowledgements

This study was funded by the Deutsche Forschungsgemeinschaft (DFG, German Research Foundation) – Project number 414265976 – TRR 277.

Literaturverzeichnis

Afkhami, Shahriar; Dabiri, Mohammad; Piili, Heidi; Björk, Timo (2021): Effects of manufacturing parameters and mechanical post-processing on stainless steel 316L processed by laser powder bed fusion. In: *Materials Science and Engineering: A* 802, S. 140660. DOI: 10.1016/j.msea.2020.140660.

AS, S.; SKALLERUD, B.; TVEITEN, B. (2008): Surface roughness characterization for fatigue life predictions using finite element analysis. In: *International Journal of Fatigue* 30 (12), S. 2200–2209. DOI: 10.1016/j.ijfatigue.2008.05.020.

Brust, A. F.; Niezgoda, S. R.; Yardley, V. A.; Payton, E. J. (2019): Analysis of Misorientation Relationships Between Austenite Parents and Twins. In: *Metall and Mat Trans A* 50 (2), S. 837–855. DOI: 10.1007/s11661-018-4977-5.

Celada-Casero, Carola; Sietsma, Jilt; Santofimia, Maria Jesus (2019): The role of the austenite grain size in the martensitic transformation in low carbon steels. In: *Materials & Design* 167, S. 107625. DOI: 10.1016/j.matdes.2019.107625.

Diller, Johannes; Auer, Ulrich; Radlbeck, Christina; Mensinger, Martin; Krafft, Frank (2020): Einfluss der Abkühlrate auf die mechanischen Eigenschaften von additiv gefertigten Zugproben aus 316L. In: *Stahlbau* 89 (12), S. 970–980. DOI: 10.1002/stab.202000034.

Diller, Johannes; Rier, Lukas; Siebert, Dorina; Radlbeck, Christina; Krafft, Frank; Mensinger, Martin (2022): Cyclic plastic material behavior of 316L manufactured by laser powder bed fusion (PBF-LB/M). In: *Materials Characterization* 191, S. 112153. DOI: 10.1016/j.matchar.2022.112153.

Gor, Meet; Soni, Harsh; Wankhede, Vishal; Sahlot, Pankaj; Grzelak, Krzysztof; Szachgluchowicz, Ireneusz; Kluczyński, Janusz (2021): A Critical Review on Effect of Process Parameters on Mechanical and Microstructural Properties of Powder-Bed Fusion Additive Manufacturing of SS316L. In: *Materials (Basel, Switzerland)* 14 (21). DOI: 10.3390/ma14216527.

Guo, Ning; Sun, Chaoyang; Fu, Mingwang; Han, Mingchuan (2017): Misorientation-Dependent Twinning Induced Hardening and Texture Evolution of TWIP Steel Sheet in Plastic Deformation Process. In: *Metals* 7 (9), S. 348. DOI: 10.3390/met7090348.

Hooper, Paul A. (2018): Melt pool temperature and cooling rates in laser powder bed fusion. In: *Additive Manufacturing* 22, S. 548–559. DOI: 10.1016/j.addma.2018.05.032.

ITOGA, Hisatake; TOKAJI, Keiro; NAKAJIMA, Masaki; KO, Haeng-Nam (2005): Effects of Notch and Surface Roughness on Long Life Fatigue Behaviour in High Strength Steels. In: *J. Soc. Mat. Sci., Japan* 54 (12), S. 1249–1254. DOI: 10.2472/JSMS.54.1249.

Liu, Jiangwei; Song, Yanan; Chen, Chaoyue; Wang, Xiebin; Li, Hu; Zhou, Chang'an et al. (2020): Effect of scanning speed on the microstructure and mechanical behavior of 316L stainless steel fabricated by selective laser melting. In: *Materials & Design* 186, S. 108355. DOI: 10.1016/j.matdes.2019.108355.

Ravi Kumar, B. (2010): Influence of crystallographic textures on tensile properties of 316L austenitic stainless steel. In: *J Mater Sci* 45 (10), S. 2598–2605. DOI: 10.1007/s10853-010-4233-x.

Schoß, Volker (2000): Martensische Umwandlung und Ermüdung austenitischer Edelstähle, Gefügeveränderungen und Möglichkeiten der Früherkennung von Ermüdungsschädigungen. Online verfügbar unter http://slubdd.de/katalog?TN_libero_mab2)500063900.

Solberg, Klas; Guan, Shuai; Razavi, Seyed Mohammad Javad; Welo, Torgeir; Chan, Kang Cheung; Berto, Filippo (2019): Fatigue of additively manufactured 316L stainless steel: The influence of porosity and surface roughness. In: *Fatigue Fract Eng Mater Struct* 42 (9), S. 2043–2052. DOI: 10.1111/ffe.13077.

Wegst, C. W. (2001): Stahlschlüssel. 2001. 19. vollständig neu bearbeitete und erweiterte Auflage 2001. Marbach: Verl. Stahlschlüssel Wegst GMBH.

Yakout, Mostafa; Elbestawi, M. A.; Veldhuis, Stephen C. (2019): Density and mechanical properties in selective laser melting of Invar 36 and stainless steel 316L. In: *Journal of Materials Processing Technology* 266, S. 397–420. DOI: 10.1016/j.jmatprotec.2018.11.006.